Ab initio electric-field gradients and electron densities at ^{27}Al, ^{57}Fe, and ^{67}Zn in the spinels $ZnAl_2O_4$ and $ZnFe_2O_4$

D. W. Mitchell* and T. P. Das
Department of Physics, The State University of New York at Albany, Albany, New York 12222

W. Potzel, W. Schiessl, H. Karzel, M. Steiner, M. Köfferlein, U. Hiller, and G. M. Kalvius
Physik-Department E15, Technische Universität München, D-85747 Garching, Germany

A. Martin
Friedrich-Schiller-Universität, Institut für Anorg. und Analyt. Chemie, D-07743 Jena, Germany

W. Schäfer and G. Will
Mineralogisches Institut der Universität Bonn, D-53115 Bonn, Germany

I. Halevy and J. Gal
Ben-Gurion University and Nuclear Research Center Negev, 84190 Beer-Sheva, Israel
(Received 6 July 1995)

The first-principles all-electron Hartree-Fock cluster procedure is applied to the spinels $ZnAl_2O_4$ and $ZnFe_2O_4$ for the pure spinels, Zn^{2+} and Fe^{3+} substituted for Al^{3+} in $ZnAl_2O_4$, and when Zn^{2+} is substituted for Fe^{3+} in $ZnFe_2O_4$. Electric-field gradients (EFG's) are calculated for the nuclei at the *B* sites using clusters which involve the *B* site cation and its six nearest-neighbor oxygens. The rest of the solid is included by considering all sites outside the cluster as point ions. The calculated EFG's agree well with the available nuclear quadrupole interaction data. For the impurity systems, the possibility of impurity-induced lattice relaxation is not included. However, the concordance found between theoretical and experimental ^{67}Zn nuclear quadrupole coupling constants (e^2qQ) indirectly suggests that the relaxation due to the presence of the defect is relatively small. For ^{57}Fe and ^{67}Zn at the *B* site, the ratios of the main component V_{zz} of the EFG's, $V_{zz}[ZnAl_2O_4]/V_{zz}[ZnFe_2O_4]$, agree very well with the experimentally determined ratios $e^2qQ[ZnAl_2O_4]/e^2qQ[ZnFe_2O_4]$. This is significant because these ratios are independent of the nuclear quadrupole moment Q. Combined with the good agreement found between theoretical and experimental results for ^{27}Al and ^{67}Zn, the present calculations suggest a value for $Q(^{57}\text{Fe})\approx 0.20$ b. Electron densities are calculated at ^{57}Fe and ^{67}Zn. The ^{57}Fe magnetic hyperfine field is calculated, and very good agreement is obtained with the experimental result for $ZnFe_2O_4$. Correcting the Hartree-Fock results for many-body and relativistic effects is important. The magnetic moment of ^{57}Fe in $ZnFe_2O_4$, estimated from the Mulliken population analysis, is found to be $4.8\mu_B$, somewhat larger than the experimental moment of $4.2\mu_B$. Charge densities at the zinc nucleus are calculated at the *A* sites for the pure spinels, and for the *B* sites when zinc is a substitutional defect. Our calculations suggest that for ^{67}Zn-Mössbauer spectroscopy contributions to the center shift from the second-order Doppler effect are significant in oxide spinels.

I. INTRODUCTION

Oxide spinels comprise a very large group of structurally related compounds,[1–4] many of which are of considerable technological[2,4] or geological[3,5] significance. Spinels exhibit a wide range of electronic and magnetic properties,[4] including superconductivity[6] in $LiTi_2O_4$. Many naturally occurring spinels are common accessory minerals, including spinel ($MgAl_2O_4$) and magnetite (Fe_3O_4). The iron-containing spinels are of technological importance due primarily to their magnetic and insulating properties. Also, the thermodynamic properties of silicate polymorphs including those with the spinel structure are of current geophysical interest[5] due to their possible importance in the mechanism of deep focus earthquakes and importance as a major mantle constituent. A recent review of oxide spinel research, especially studies involving ^{57}Fe Mössbauer spectroscopy, is available in the literature.[4]

Nearly all spinels belong to the space group $Fd3m$ (O_h^7) though some lower symmetry spinels also exist.[4] Spinels are isostructural with the mineral spinel $MgAl_2O_4$, crystallize in a face-centered-cubic lattice and contain eight molecules per unit cell. There are two kinds of voids in such an arrangement; those tetrahedrally and those octahedrally coordinated by oxygens. The tetrahedrally coordinated and octahedrally coordinated positions are called *A* sites and *B* sites, respectively. This structure is described in detail by Gorter[2] and Hill, Craig, and Gibbs.[3] The unit cell is shown in Fig. 1. The spinel structure (space group $Fd3m$) is characterized by just two parameters, the lattice constant *a* and the oxygen position parameter *u* of the 32 (*e*) positions. In the ideal spinel structure, the oxygen anions form a perfect face-centered-cubic sublattice for which $u=\frac{3}{8}=0.375$. However,

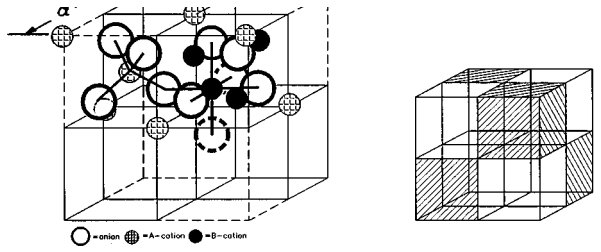

FIG. 1. Cubic unit cell of the spinel structure with lattice constant a. Left: A cations are tetrahedrally, B cations octahedrally coordinated by anions. Right: the A sites are at the center of the open cubes and at the fcc positions of the unit cell. All B sites are contained within the shaded cubes.

in most spinels $u \neq 0.375$, which leads to a trigonal distortion of the octahedron of oxygens surrounding the B site along [111], while the A site retains its cubic symmetry.

There are two basic types of spinels,[1–4] the so-called normal and inverse spinels. The normal spinels, of which $ZnAl_2O_4$ and $ZnFe_2O_4$ are typical examples, have the general formula $(X)[Y_2]O_4$, where X and Y are divalent and trivalent ions, respectively. The ( ) and [ ] refer to the eight tetrahedrally coordinated A sites and 16 octahedrally coordinated B sites, respectively, within the cubic unit cell. In the normal spinel structure all of the divalent cations are at the A sites, and all of the trivalent cations are at the B sites. Inverse spinels can be described by the formula $(Y)[XY]O_4$. All of the X ions and one-half of the Y metal ions have switched places compared to the normal spinel structure.

The two spinels investigated here, $ZnAl_2O_4$ (gahnite) and $ZnFe_2O_4$ (franklinite) belong to the normal spinel structure. This is largely a consequence of electrostatics, which predicts a lower Madelung energy for normal than for inverse spinels when the metal ions are divalent and trivalent species, as well as the strong preference of Zn for tetrahedral coordination.[1] This latter effect may be understood to be due to the full Zn($3d$) shell for the Zn^{2+} ion, leading Zn preferentially to form sp^3 hybrid bonds with the oxygen anions.

This study deals primarily with the origin of the nuclear quadrupole coupling constants (e^2qQ) at the B sites in normal spinels. The point symmetry[7] of the eight tetrahedral A sites is cubic $\bar{4}3m$ (T_d), while that of the 16 octahedral B sites is trigonal $3m$ (D_{3d}). Hence for normal spinels a zero electric-field gradient is expected at the cubic A site.[7–9] The electric-field gradient (EFG) tensor at the B site is axially symmetric with the maximum component V_{zz} of the EFG tensor in the principal axis system directed along the [111] direction.[7–9]

Until now only point multipole models have been used to study the electric-field gradients in spinels. Previous investigations of normal spinels have convincingly shown[7–9] that one must include at least the dipole moments on the oxygens to obtain even qualitative agreement with experiment. A monopole-only calculation for the EFG at the B site in normal spinels gives a qualitatively incorrect description of the EFG. Therefore, we have undertaken a first-principles study of the sign and magnitude of V_{zz} at the B site in spinels by the Hartree-Fock cluster procedure,[10–16] a method which has been shown to be successful in determining hyperfine properties[11–16] in other ionic systems. The spinels we have chosen to describe in detail here are $ZnAl_2O_4$ and $ZnFe_2O_4$. The lattice parameters which we measured by neutron diffraction are for $ZnAl_2O_4$, where $a=8.0813(3)$ Å and $u=0.3887(2)$; and for $ZnFe_2O_4$, where $a=8.4599(5)$ Å and $u=0.3845(2)$. These spinels not only have e^2qQ measured for the pure systems, namely for Al^{3+} in $ZnAl_2O_4$ and Fe^{3+} in $ZnFe_2O_4$, but also for the cases when Zn^{2+} or Fe^{3+} (^6S) substitute as an impurity for Al^{3+} in $ZnAl_2O_4$ and when Zn^{2+} substitutes for Fe^{3+} in $ZnFe_2O_4$. Table I summarizes the experimentally determined quadrupole coupling constants. Here we present results of theoretical calculations for all of these cases. The impure systems are treated by simply substituting the impurity for the ion in the pure compound without allowing for impurity-induced lattice relaxation. Information about the extent of the lattice relaxation is derived by comparing the theoretical and experimental results. This work greatly extends our earlier study[16] on ^{27}Al and ^{67}Zn nuclear quadrupole interactions in $ZnAl_2O_4$ and, in particular, includes a consideration of the following: the use of more extensive basis sets, an estimate of the contribution of the oxygen dipoles external to the cluster, and the investigation of Fe^{3+} in $ZnAl_2O_4$ as well as Fe^{3+} and Zn^{2+} in $ZnFe_2O_4$.

TABLE I. Experimental nuclear quadrupole coupling constants (e^2qQ) for various B-site ions in $ZnAl_2O_4$ and $ZnFe_2O_4$.

Spinel	B site nucleus	e^2qQ (MHz)	Method
$ZnAl_2O_4$	^{27}Al	± 3.68	N.M.R.[a,b]
$ZnAl_2O_4$	^{57}Fe	-18.1 (1)	Mössbauer[a]
$ZnAl_2O_4$	^{67}Zn	-11.4 (1.1)	Mössbauer[c,d]
$ZnFe_2O_4$	^{57}Fe	-7.74 (2)	Mössbauer [e]
$ZnFe_2O_4$	^{67}Zn	-6.0 (9)	Mössbauer [d]

[a]Reference 17.
[b]The sign of e^2qQ (^{27}Al) is experimentally undetermined (Ref. 17).
[c]References 18 and 19.
[d]Reference 19.
[e]Reference 8.

II. THEORETICAL PROCEDURE

The all-electron self-consistent Hartree-Fock cluster procedure has been used with success for the investigation of nuclear quadrupole interactions in a number of ionic crystals,[11–16] including ^{27}Al and ^{67}Zn at the Al site[16] in the spinel $ZnAl_2O_4$, and high-T_c systems,[14,15] and for the study of magnetic hyperfine interactions.[11,14] This method has also been successfully applied to the calculation of ^{67}Zn isomer shifts.[20]

The Hartree-Fock cluster procedure has been described in detail elsewhere,[10–16,20] and only a brief summary is given here involving some points especially pertinent for the present investigations. In this method, which utilizes the Hartree-Fock-Roothaan variational approach,[21] the solid-state system is simulated[22] by a finite number of ions, which we call a cluster, with the ion whose properties are being investigated at the center. The number of ions chosen in such calculations is based on a compromise between accuracy and

TABLE II. Madelung potentials V_m at the A, B, and oxygen sites in $ZnAl_2O_4$ and $ZnFe_2O_4$.

Spinel	Site	V_m $(e\text{Å}^{-1})$
$ZnAl_2O_4$	Zn^{2+}	-1.7814
	Al^{3+}	-2.4839
	O^{2-}	$+1.8106$
$ZnFe_2O_4$	Zn^{2+}	-1.8070
	Fe^{3+}	-2.2954
	O^{2-}	$+1.7236$

practicability. The influence of the rest of the lattice is incorporated by including in the Hartree-Fock potential for the electrons in the cluster the potential due to the ions outside the cluster, considering their influence to be described as those due to point charges. In this way the Madelung potential is incorporated in the all-electron Hartree-Fock cluster procedure by replacing the ions comprising the surroundings of the cluster with their ionic point charges out to 15 Å from the central atom. The charges on the ions in the outermost shells are adjusted to exactly reproduce the Madelung potential of the true solid at all cluster atoms, as well as requiring that charge neutrality is maintained for the entire system of cluster plus point charges. The incorporation of this potential due to the rest of the lattice not only allows one essentially to include the whole crystal in calculations, but also provides the important stabilization potential necessary to localize the electron distribution in diffuse negative ions like O^{2-}. The Madelung potential at all lattice sites for the lattice parameters given in Sec. I are listed in Table II. These potentials have been calculated using the method of Nijboer and DeWette.[23]

For our B site V_{zz} calculations, clusters $(AlO_6)^{9-}$, $(FeO_6)^{9-}$, and $(ZnO_6)^{10-}$ are utilized. Using the lattice parameters given in Table I, the Al-O nearest-neighbor distance in $ZnAl_2O_4$ is 1.9160 Å. The Fe-O nearest-neighbor distance in $ZnFe_2O_4$ is 2.0378 Å. The choice of a charge of -10 for the Zn cluster is based on the experimental observation that no transferred hyperfine field is detected[18,19] at ^{67}Zn for Zn^{2+} at the B site in $ZnAl_2O_4$ from Mössbauer measurements. This indicates that a divalent Zn^{2+} ion with no magnetism and hence a closed-shell cluster with zero spin is the correct choice,[16] although Zn^{2+} at the B site may represent a charged defect.

Contracted Gaussian-type basis functions (GTF's) are employed in these variational Hartree-Fock calculations.[24,25] The chosen basis sets are of double-zeta plus polarization quality.[24] For oxygen we have used the basis set of Dunning,[26] which is optimized for neutral O. Our earlier experience[13] regarding the ^{67}Zn nuclear quadrupole interaction in ZnO demonstrated that both basis sets optimized for the neutral oxygen atom and basis sets optimized for O^{2-} in a Watson sphere potential give similar results for calculated electric-field gradients, provided they are flexible enough. In all the basis sets used in the present work, the most diffuse exponents have been uncontracted from the rest of the basis set for greatest variational flexibility.[25] The contraction scheme of the oxygen basis in the terminology that is commonly used[25] for quantum chemical calculations is $9s$, $5p$, and $1d$ primitive GTF's contracted to $4s(6111)$, $2p(41)$, and $1d(1)$ basis functions. For zinc and iron, we have used Wachters's full double-zeta basis set[27] optimized for neutral atoms but augmented with a diffuse p exponent[28] (exponents of 0.3 and 0.2 for Zn and Fe, respectively). The contraction schemes of the Zn and Fe basis sets are each $14s$, $10p$, and $5d$ primitive GTF's contracted to $8s(62111111)$, $6p(511111)$, and $2d(41)$ basis functions. Finally, for aluminum we have used the double-zeta basis set of Dunning[26] optimized for the neutral atom but with the most diffuse s and p exponents removed since the range of these exponents, defined as $(2\times\text{exponent})^{-1/2}$, is approximately twice the range of the most diffuse (smallest) oxygen basis set exponents. In order to have a balanced basis set and to obtain physically meaningful Mulliken populations,[29] the most diffuse s and p exponents ($s_{\text{exp}}=0.078$ and $p_{\text{exp}}=0.076$) have been removed from the Al basis set. While they are important for the free neutral Al atom, the Al^{3+} cation has a much more restricted charge distribution. Furthermore, the crystalline environment localizes the electrons for both the cations and anions. The most diffuse GTF s and p exponents of the Al basis set are now 0.202 and 0.304, respectively. The contraction scheme of the Al basis set is $11s$, $7p$, and $1d$ primitive GTF's contracted to $5s(53111)$, $4p(4111)$, and $1d(1)$ basis functions. The exponents of the single Gaussian d-polarization functions for oxygen and aluminum are taken from Huzinaga[25] with exponents of 1.15 and 0.20 for oxygen and aluminum, respectively.

The oxygen and zinc basis sets utilized here have been used in earlier studies including ^{67}Zn nuclear quadrupole interactions and isomer shifts in ZnF_2 and the zinc chalcogenides.[20] The iron basis set is a similar one employed in the study of ^{57}Fe hyperfine properties in α-Fe_2O_3 (Ref. 11) and the ^{57}Fe isomer shift in K_3FeF_6.[30]

Once the molecular-orbital wave functions ψ_μ for the cluster are determined self-consistently the components of the EFG tensor site can be calculated using the expression[15]

$$V_{ij}=V_{ij}^N+V_{ij}^e+V_{ij}^{\text{ext}}, \tag{1}$$

where V_{ij}^N and V_{ij}^e correspond to the contributions to the ij component of the EFG tensor from the nuclear charges ξ_N and the electrons in the cluster (the sum of which we call the cluster V_{zz}) while V_{ij}^{ext} represents the contribution due to the point charges external to the cluster as well as oxygen dipole moments whose influence is incorporated by a procedure described below. By the inclusion of the nearest neighbors in the cluster, covalency, and charge-transfer effects on V_{ij} are included in a first-principles manner.

The external contribution V_{ij}^{ext} representing the contribution to the EFG tensor from the external monopoles and higher multipoles is given by

$$V_{ij}^{\text{ext}}=V_{ij}^{(0)\text{ext}}+(1-\gamma_\infty)[V_{ij}^{(1)\text{ext}}+V_{ij}^{(2)\text{ext}}+\cdots], \tag{2}$$

where $V_{ij}^{(0)\text{ext}}$ is the EFG contribution from the point charges (monopoles) external to the cluster. Since our Hartree-Fock procedure is an all-electron calculation, and the monopoles are included in the Hartree-Fock Hamiltonian explicitly, the core and valence electrons in the ions are all perturbed by the sources of EFG internal and monopoles external to the cluster. Therefore, Sternheimer antishielding effects[31,32] are di-

rectly included without the need to introduce antishielding factors γ_∞ for the monopoles. This is not true, however, for the dipoles and quadrupoles, whose lattice contributions[33,34] to the EFG tensor are defined as $V_{ij}^{(1)\text{ext}}$ and $V_{ij}^{(2)\text{ext}}$, respectively, in Eq. (2). Since these higher-order multipoles are not included in the embedding lattice external to the cluster, the antishielding factor γ_∞ is needed for their contributions. However, we find that the dipole contribution of the lattice external to the nearest-neighbor octahedron of oxygens to the B site is just around 15% of the total dipole contribution. This suggests that nearly all of the dipole effects to the B-site EFG are contained within the cluster itself. In addition, nearly all of the effects of the higher multipoles are included within the cluster. For instance, the monopoles, dipoles, and quadrupoles make contributions to V_{ij} which fall off as d^{-3}, d^{-4}, and d^{-5}, respectively, where d is the distance from the central B site nucleus. We therefore choose to neglect multipoles higher than the oxygen dipoles, and estimate the contribution due to the oxygen dipoles from the point-dipole model. This somewhat reduces the beauty of the cluster method by reintroducing Sternheimer antishielding factors[31,32] and the oxygen dipole polarizability α_D, but allows an estimate of the magnitude of such contributions. Since these contributions turn out to be small, we did not make an effort to perform more accurate calculations such as determining the oxygen dipole moment from cluster investigations. The incorporation of the effects of the potential due to dipoles on the cluster wave functions, to avoid having to employ antishielding parameters, would be rather time consuming, but would be useful to attempt in the future.

In the subsequent sections of this paper, the results for the B-site nuclear quadrupole interactions are presented and discussed. The nuclear quadrupole interactions in the perfect spinel system of Al^{3+} in $ZnAl_2O_4$ are described first, followed by ^{67}Zn and ^{57}Fe nuclear quadrupole interactions in $ZnAl_2O_4$ and $ZnFe_2O_4$. Finally, the results regarding ^{57}Fe magnetic hyperfine interactions and ^{57}Fe isomer shifts at the B site and ^{67}Zn isomer shifts at the A and B sites are given and compared with experimental measurements.

To gain additional insight into the origin and sign of the EFG, self-consistent molecular orbitals are used to extract approximate individual atomic-orbital contributions to the EFG. To accomplish this all self-consitent orbital coefficients are set to zero except the ones corresponding to basis sets centered on the atom (Zn, Fe, Al, or O) with angular momentums (s, p, or d) we are interested in. Hence, for example, the O(s,p,d) atomic orbital contribution is obtained by setting all molecular-orbital coefficients belonging to metal ion-centered basis sets equal to zero, then evaluating the appropriate matrix elements. This procedure is an approximation, since overlap terms between the various orbitals are not indicated, although they are, of course, taken into account in the self-consistent calculations. Fortunately, these overlap terms turn out to make only small contributions to the EFG's in all systems studied here.

In all of the compounds investigated, we find that the electric-field-gradient tensor at the B-site nucleus is axially symmetric, and therefore the asymmetry parameter $\eta=0$ and only the maximum component of the electric-field-gradient tensor V_{zz} in the principal axis system needs to be considered further. We also find that for all cases to be studied, the sign of V_{zz} is negative, and the direction of V_{zz} is in the [111] crystal direction. All of these results are in agreement with the experimental measurements.

TABLE III. V_{zz} for the $(AlO_6)^{9-}$ cluster in $ZnAl_2O_4$.

External charges	Al basis set[a]	O basis set[b]	Al Mulliken charge	Cluster V_{zz} (a.u.)
[c]	$5s4p$	$4s2p$	$+2.46$	-0.1134
[c]	$5s4p$	$4s2p1d$	$+2.47$	-0.1255
[c]	$5s4p1d$	$4s2p$	$+2.28$	-0.1301
[c]	$5s4p1d$	$4s2p1d$	$+2.31$	-0.1384
[d]	$5s4p1d$	$4s2p1d$	$+2.25$	-0.1401

[a]Aluminum d-polarization function (exponent 0.2).
[b]Oxygen d-polarization function (exponent 1.15).
[c]The external charges are $Zn^{1.53+}Al_2^{2.30+}O_4^{1.53-}$.
[d]The external charges are formal charges, $Zn^{2+}Al_2^{3+}O_4^{2-}$.

III. RESULTS AND DISCUSSION

A. ^{27}Al nuclear quadrupole interaction in $ZnAl_2O_4$

This compound corresponds to the pure spinel, and is especially suited for our study for the following reasons: (1) Al^{3+} is an S-state ion; (2) the quadrupole moment, Q, of ^{27}Al is fairly well established, and the same holds for ^{67}Zn but not for ^{57}Fe; (3) γ_∞ (^{27}Al)≈ -2.6 is small; and (4) this system corresponds to the pure crystal. Reason (1) is also true for all other ions studied here as well, which simply means that the lattice contribution to V_{zz} is dominant. S-state ions have spherically symmetric charge distributions. Uncertainties associated with impurity-induced lattice relaxation are not involved for pure crystalline systems. In addition, since γ_∞ is small for Al^{3+}, the magnitude of the dipole contribution to V_{zz}, estimated from the point-dipole model, is relatively small compared to the Zn^{2+} and Fe^{3+} cases. In conclusion, the ^{27}Al nuclear quadrupole interaction (NQI) in $ZnAl_2O_4$ can be considered an excellent benchmark case to test the electric-field gradients at B-site nuclei in spinels calculated by the Hartree-Fock cluster procedure.

The EFG at the Al nucleus in $ZnAl_2O_4$ has been calculated for the $(AlO_6)^{9-}$ clsuter using different basis sets in order to determine the influence of d-polarization functions on the Al and O basis sets. These basis sets are the sp portions of the Dunning basis sets,[26] as described in Sec. II. In Table III results of these calculations are given for the following cases: both the O and Al basis sets have no d-polarization functions; one but not the other species has a d-polarization function; and all atoms have basis sets augmented with single Gaussian d-polarization functions (exponents of 1.15 and 0.2 for O and Al, respectively). In order to test the sensitivity of the final results to the chosen external charges, two different sets of point charges have been used for the ions external to the central $(AlO_6)^{9-}$ cluster. These are when the external point ions are formal charges (i.e., $+2$, -2, and $+3$ for Zn, O, and Al) corresponding to total ionicity, and when these charges are scaled by a constant factor 2.3/3.0 (i.e., approximately $+1.53$, -1.53, and $+2.3$ for the external Zn, O, and Al sites, respectively). This scaling of the external charge magnitudes is based on the

charge of the central Al atom in the $(AlO_6)^{9-}$ cluster obtained from Mulliken population analysis for the case when d-polarization functions are on both Al^{3+} and O^{2-} ions within the clusters. As seen from Table III, for this best basis set situation the Al Mulliken charge came out to be about $+2.3$, which is smaller than the formal Al^{3+} charge. The rationale for the use of a uniform scaling factor is that since the central Al atom is best described within the $(AlO_6)^{9-}$ cluster, the Al Mulliken charge is more accurate than the oxygen charge, the former being fully coordinated by its nearest-neighbor oxygens within the cluster. Reducing the external charges from thier formal totally ionic values has some physical grounds, in that convalency reduces the charges somewhat from the formal ionic values, and that the Mulliken charges reflect this covalency. A detailed study concerning possible uncertainties associated with the choice of external point-charge magnitude is presented elsewhere.[35]

In Table III, the use of formal ionic charges in the embedding lattice is presented only for one case, namely when d-polarization functions are centered on both the Al and O ions within the cluster. As seen from Table III, the use of formal or Mulliken (scaled) charges for the external ions gives very similar results for the Al Mulliken population and the V_{zz} originating from the nuclei and electrons within the $(AlO_6)^{9-}$ cluster. The relative closeness of the Mulliken charges is indicative of the fast convergence of the process of charge iteration to self-consistency of the external charge values. In this procedure, the external ions are replaced by the Mulliken charges; then the Hartree-Fock cluster calculation is repeated until the external Al charge equals the Mulliken Al charge within the cluster. The calculated V_{zz} from within the cluster is very close (-0.140 and -0.138 a.u. for formal and scaled charges in the external lattice, respectively). This is likely due to the dominance of the valence Al($3p$) contribution to V_{zz}, which is based on covalency between the Al-O bond. Covalency effects on V_{zz} are relatively insensitive to the embedding lattice. The lattice EFG at the Al nucleus due to the point ions external to the cluster mainly influences the core Al($2p$) electrons through Sternheimer antishieldinglike effects,[31,32] which are small for Al^{3+} due to the relative smallness of γ_∞ for Al^{3+}. These effects are given a more quantitative meaning in Sec. III B, when individual contributions to the EFG at the Al nucleus are discussed. It is apparent from Table III that the V_{zz} cluster becomes more negative as the basis sets are augmented with d-polarization functions. Comparing the case when there are no d-polarization functions on either Al or O to the case when both types of atoms have d-polarization functions, one observes that the cluster V_{zz} is reduced by 22% and that the Al Mulliken charge decreases slightly. The smaller Al Mulliken charge is indicative of a more covalent Al-O bond. However, the small difference between $+2.5$ and $+2.3$ charges should not be considered significant due to the uncertainties associated with the use of the Mulliken population analysis in the first place.

Using the polarized Gaussian basis sets described earlier with external point charges scaled uniformly by 2.3/3.0 from the formal values gives a value of V_{zz} at the Al nucleus of -0.1384 a.u. for the electrons and nuclei within the $(AlO_6)^{9-}$ cluster. As Table IV shows, individual contributions due to the electrons and nuclei within the cluster come out as -0.3781 a.u. and $+0.2397$, respectively. The contribution due to the external monopoles is $+0.0424$ a.u. The most important higher-order multipole is the contribution to the Al-site EFG from the dipoles on the oxygen sites. The dipole moments of the ions at the A and B sites vanish due to crystallographic symmetry. As discussed earlier, most of the oxygen dipole contribution is already contained within the cluster. However, there is a residual contribution from the oxygen anions external to the $(AlO_6)^{9-}$ cluster. To estimate the dipole contribution, the value of $\alpha_D \approx 0.4$ Å^3 has been chosen for the oxygen dipole polarizability. This is derived from a best fit of the experimental EFG to the EFG obtained by the point-charge–point-dipole model.[7–9,36] This value for α_D is in good agreement with the results of Kirsch, Gerard, and Wautelet,[9] who employed a similar method. The contribution to V_{zz}^{latt} at the Al site due to the dipoles external to the cluster is -0.0025 a.u. Since external dipoles are not included in the Hartree-Fock Hamiltonian, this contribution must be multiplied by $(1-\gamma_\infty) \approx 3.6$ for the Al^{3+} ion.[37] Therefore, the contribution to V_{zz} due to the external dipoles is approximately -0.0091 a.u. The external dipole contribution is thus quite small compared to either the external monopoles or nuclei and electrons within the cluster. The total V_{zz} at the Al site is the sum of the V_{zz} cluster and the external monopoles and dipoles, which comes out to a total of -0.1051 a.u. In order to make a comparison with experimental e^2qQ, a value of the quadrupole moment for ^{27}Al must be used. There are two values for $Q(^{27}\text{Al})$ in the litera-

TABLE IV. Contributions to V_{zz} in atomic units from various sources for Al^{3+} at the B site in $ZnAl_2O_4$.

Contribution	Al^{3+}: $ZnAl_2O_4$ V_{zz}
nuclear (from six nearest-neighbor O)	$+0.2397$ a.u.
total electronic [from $(AlO_6)^{9-}$ cluster]	-0.3781
cluster total	-0.1384
O(s,p,d)	-0.293
Al(d)	-0.0004
Al($2p$)	$+0.014$
Al($3p$)	-0.121
Al(p)$_{\text{total}}$	-0.107
monopoles external to cluster [a]	$+0.0424$
dipoles external to cluster[a,b]	-0.0091
total V_{zz}	-0.1051 a.u. = -1.02×10^{17} V/cm^2

[a] Mulliken charges are used for the ionic charges outside the cluster.
[b] $\gamma_\infty(Al^{3+}) = -2.6$ and oxygen dipole polarizability $\alpha_D = 0.4$ Å^3. γ_∞ is needed for the dipole contribution, since external dipoles are not included in the Hartree-Fock Hamiltonian; the choice of $\alpha_D = 0.4$ Å^3 is from a best fit of the experimental field gradient and theoretical gradient within the point-dipole model.

ture, derived at by a comparison of atomic many-body calculations for V_{zz} with experimental e^2qQ. These are 0.165(2) b (Ref. 38) and 0.1402(10) b,[39] with the smaller of the two the most recently derived result. We find values of e^2qQ for the ^{27}Al nucleus in $ZnAl_2O_4$ of -4.07 and -3.46 MHz using, respectively, $Q(^{27}\mathrm{Al})=0.165$ and 0.1402 b. These results are in excellent agreement with the experimental ^{27}Al nuclear-magnetic-resonance measurement[17] of ± 3.68 MHz (sign undetermined). If instead, the theoretical total V_{zz} of -0.1051 a.u. is combined with the experimental e^2qQ of ± 3.68 MHz, one obtains a nuclear quadrupole moment $Q(^{27}\mathrm{Al})$ of about 0.15 b.

In order to obtain additional information on the origin of the EFG and especially its sign, the self-consistent molecular orbitals are used to extract individual atomic-orbital contributions to the EFG. This is done by retaining only the molecular-orbital coefficients whose center (Al or O) and angular momentum (s,p,d) we are interested in (see Sec. II). The results of this procedure are also summarized in Table IV. The contributions to V_{zz} at the Al site due to the cluster electrons from O(s,p,d), Al(p), and Al$(3d)$ orbitals are -0.293, -0.107, and -0.0004 a.u., respectively. The contribution from O(s,p,d) orbitals (-0.293 a.u.) is largely compensated for by the nuclear contribution ($+0.2397$ a.u.) of the six nearest-neighbor O. The Al(p) contribution of -0.107 a.u. is nearly equal to the total V_{zz} of -0.105 a.u. The Al$(3d)$ orbitals contribute very little to the B-site V_{zz}. However, as seen from Table III the inclusion of d-polarization functions to the Al basis set changes V_{zz} noticeably. The possible origin of this difference is that the Al$(3d)$ orbitals influence V_{zz} indirectly by polarizing the Al$(3p)$ orbitals. The dominant Al(p) contribution of V_{zz} is the result of $+0.014$ a.u. from the core Al$(2p)$ and of -0.121 a.u. from the valence Al$(3p)$ electrons. We can conclude that the origin of the V_{zz} is due mainly to the valence Al$(3p)$ electrons. The sign of V_{zz} is predicted to be negative due to the large negative contribution from the valence Al $(3p)$ electrons which is about nine times greater in magnitude than a smaller positive contribution from the core Al $(2p)$ orbitals. These results show the importance of covalency effects in the calculation of V_{zz} for $ZnAl_2O_4$, and explain the relative insensitivity of the EFG to the external charges, the latter influencing primarily the Sternheimer-type polarization contributions such as the one arising from the Al core $2p$ electrons.

There are several sources of uncertainties to consider in the above calculations. These include finite cluster size, error in external multipoles, neglect of many-body contribution, and basis set limitations. The many-body contributions to V_{zz} is likely small. This is due to the fact that all ions within $ZnAl_2O_4$ are S-state ions with completely filled shells. Brillouin's theorem, which states that for closed-shell molecules the matrix elements of one-electron operators connecting singly excited configurations to the ground state are zero, is then valid. Therefore, the leading nonvanishing many-body contributions to V_{zz} would come from doubly excited configurations. Also, many-body effects on V_{zz} are expected to be small, since one is dealing with basically an ionic compound for which the electrons are usually localized on particular ions. Finally, first-principle many-body perturbation theory calculations on Fe^{2+} and Fe^{3+} ions,[40,41] and recent many-body calculations[42] on small iron-containing molecules, have demonstrated the relative unimportance of many-body effects on the electric-field gradient or the isomer shift. In regards to cluster size, previously[16] we partially tested the convergence of the calculated EFG with respect to the cluster size by replacing the six second-nearest-neighbor Al^{3+} point charges by total cation pseudopotentials[43] with no basis functions centered on them, in effect increasing the quantum-mechanical size of the cluster to $(AlO_6Al_6)^{9+}$. The result of this expansion increased V_{zz} at the Al site by only 0.0003 a.u. compared to the original $(AlO_6)^{9-}$ cluster. The use of total cation pseudopotentials replacing the Al^{3+} cores accounts for the repulsive Pauli interaction between the two nearest-neighbor Al^{3+} ions and the nearest-neighbor oxygen anions. However, this short-range repulsive interaction may not be enough to test for cluster size convergence, since covalency and charge-transfer effects are not included. Nonetheless, at least for the pure spinel, the $(AlO_6)^{9-}$ cluster appears to be adequate for a quantitative description of the Al-site EFG.

B. ^{67}Zn and ^{57}Fe nuclear quadrupole interactions in $ZnAl_2O_4$ and $ZnFe_2O_4$

1. Comparison with experiment

The experimental e^2qQ measurements are listed in Table I. The signs of the ^{67}Zn and ^{57}Fe e^2qQ have all been experimentally determined to be negative. The ratio $e^2qQ[ZnAl_2O_4]/e^2qQ[ZnFe_2O_4]$ of the experimental e^2qQ results for a given B-site nucleus between the two different spinels is very important in that it is independent of the nuclear quadrupole moment Q and can be compared directly to the ratio of theoretically determined V_{zz} for the different spinels. With measured nuclear quadrupole coupling constants available for two different nuclei located at the same lattice site in two different compounds with the same structure, one has an unusual opportunity to test calculated electric-field gradients at these sites (see below).

Concerning Zn^{2+} at the B sites in $ZnAl_2O_4$ and $ZnFe_2O_4$, it seems likely that significant impurity-induced lattice distortion may occur due to the replacement of the smaller Al^{3+} and Fe^{3+} ions with a larger Zn^{2+} cation.[18,19] Furthermore, replacing Al^{3+} or Fe^{3+} with Zn^{2+} implies that one is also dealing with a charged defect which can cause additional lattice distortion. Nonetheless, it is still useful to obtain results for theoretical electric-field gradients in these systems without allowing for lattice distortion due to the presence of the Zn^{2+} defect. A full treatment of lattice relaxation in spinels in a first-principles manner is a major undertaking, at least in computer time.

Before discussing in detail our results regarding the Hartree-Fock cluster calculations for Zn^{2+} and Fe^{3+} at the B sites in $ZnAl_2O_4$ and $ZnFe_2O_4$, it is useful to mention the uncertainties in the accepted values for the ^{27}Al, ^{67}Zn, and ^{57}Fe nuclear quadrupole moments (Q) which are published in the literature. The nuclear quadrupole moments for ^{27}Al (Refs. 38 and 39) and ^{67}Zn (Refs. 44 and 45) are reasonably well agreed upon. For $Q(^{57}\mathrm{Fe})$, the situation appears to be far from settled.[35] The values cover the range from 0.21 b (Ref. 46) over 0.15 b (Refs. 47 and 48) to 0.082 (Ref. 49).

TABLE V. Contributions to V_{zz} in atomic units from various sources for Zn^{2+} at the B site in $ZnAl_2O_4$ and $ZnFe_2O_4$.

Contribution	Zn^{2+}: $ZnAl_2O_4$ V_{zz}	Zn^{2+}: $ZnFe_2O_4$ V_{zz}
nuclear (from six nearest-neighbor O)	+0.2397 a.u.	+0.1350 a.u.
total electronic [from $(ZnO_6)^{10-}$ cluster]	−0.5501	−0.2367
cluster total	−0.3104	−0.1016
O(s,p,d)	−0.290	−0.169
Zn(d)	−0.021	+0.013
Zn($2p$)	−0.022	−0.004
Zn($3p$)	−0.002	+0.047
Zn($4p$)	−0.260	−0.140
$Zn(p)_{total}$	−0.284	−0.097
monopoles external to cluster [a]	+0.0424	+0.0394
dipoles external to cluster[a,b]	−0.0382	−0.0579
total V_{zz}	−0.3062 a.u. = -2.98×10^{17} V/cm^2	−0.1201 a.u. = -1.17×10^{17} V/cm^2

[a]Mulliken charges are used for the ionic charges outside the cluster.

[b]$\gamma_\infty(Zn^{2+})=-14.1$, which is the free ion value (Ref. 37). γ_∞ is needed for this contribution since dipoles are not included in the embedding lattice; for $ZnAl_2O_4$ and $ZnFe_2O_4$, $\alpha_D=0.4$ and 0.8 Å^3, respectively, were used.

In Tables V and VI results are presented for Zn^{2+} and Fe^{3+} at the B sites in $ZnAl_2O_4$ and $ZnFe_2O_4$ obtained by the Hartree-Fock cluster procedure. The method used is the same as for the Al^{3+} cation in the pure spinel $ZnAl_2O_4$. The chosen cluster for the Fe^{3+} ion at the B site in $ZnAl_2O_4$ or $ZnFe_2O_4$ is $(FeO_6)^{9-}$, while for Zn^{2+} at the B site the chosen cluster is $(ZnO_6)^{10-}$. The results of Tables V and VI are for external point charges scaled uniformly by 2.3/3.0 times the formal charges. This value, as described earlier, is based on the Mulliken charge of about +2.3 obtained for Al in the $(AlO_6)^{9-}$ cluster for $ZnAl_2O_4$. The same scaling factor has also been chosen for all other clusters, which include those for the systems Zn^{2+} and Fe^{3+} at the Al site in $ZnAl_2O_4$, and for Zn^{2+} and Fe^{3+} at the Fe site in $ZnFe_2O_4$. As will be shown below, the Mulliken charges obtained for Fe^{3+} or Zn^{2+} in both spinels are fairly close, therefore giving partial justification for the use of the same scaling factor for both spinels.

For the oxygen dipole polarizability α_D, values of 0.4 and 0.8 Å^3 are chosen for $ZnAl_2O_4$ and $ZnFe_2O_4$, respectively. The estimates made here are based on a best fit between experimental and theoretical V_{zz} obtained using the point-dipole model. Hence these estimates for α_D rely on both a knowledge of Q and γ_∞. For $ZnAl_2O_4$, α_D has been obtained using the ^{27}Al e^2qQ measurements with $Q(^{27}Al)\approx0.15$ b and $\gamma_\infty=-2.6$.[37] For $ZnFe_2O_4$, due to the large uncertainty in $Q(^{57}Fe)$, the ^{67}Zn e^2qQ results have been chosen instead for comparison with the point-dipole calculations. Since the Zn and Al V_{zz}^{latt} results are similar for $ZnAl_2O_4$, it was felt that the Zn results for V_{zz}^{latt} in $ZnFe_2O_4$ should be of sufficient reliability for obtaining α_D in $ZnFe_2O_4$. The $\alpha_D\approx0.8$ Å^3 used for $ZnFe_2O_4$ is the same value as estimated by Evans, Hafner, and Weber.[8] The external dipole contributions also depend on γ_∞, for which the free-ion value $\gamma_\infty(Zn^{2+})=-14.1$ (Ref. 37) is used.

Starting first with the $ZnAl_2O_4$ results, the cluster contributes −0.3104 a.u. to V_{zz}, of which +0.2397 and −0.5501 a.u. are due to the nuclei and the electrons within the $(ZnO_6)^{10-}$ cluster, respectively. To this total one must add the contributions due to the monopoles and oxygen dipoles external to the cluster, which are +0.0424 and −0.0382 a.u., respectively. One observes that unlike the Al results, the dipole contribution to V_{zz} for Zn^{2+} at the B site is much larger. This is due to the 5.4 times greater value of $\gamma_\infty(Zn^{2+})$ compared to $\gamma_\infty(Al^{3+})$. Combining the cluster and external contributions yields a total V_{zz} of −0.3062 a.u. for Zn^{2+} at the B site in $ZnAl_2O_4$.

Moving next to Zn^{2+} at the B site in $ZnFe_2O_4$, we find that the cluster contribution to V_{zz} is −0.1016 a.u., while the contributions due to external monopoles and oxygen dipoles come out to +0.0394 and −0.0579 a.u., respectively. The total V_{zz} for Zn^{2+} in $ZnFe_2O_4$ is therefore −0.1201 a.u. The experimental results[18,19] for the coupling constants e^2qQ/h for Zn^{2+} in $ZnAl_2O_4$ and $ZnFe_2O_4$ are -11.4 ± 1.1 and -6.0 ± 0.9 MHz, respectively (see Table I).

TABLE VI. Contributions to V_{zz} in atomic units from various sources for Fe^{3+} at the B site in $ZnAl_2O_4$ and $ZnFe_2O_4$. α refers to spin-up electrons. β refers to spin-down electrons.

Contribution	Fe^{3+}: $ZnAl_2O_4$ V_{zz}		Fe^{3+}: $ZnFe_2O_4$ V_{zz}	
nuclear (from six nearest-neighbor O)	$+0.2397$		$+0.1350$	
	α electrons	β electrons	α electrons	β electrons
electronic total [a]	-0.3424	-0.2880	-0.1566	-0.1431
$O(s,p,d)$	-0.153	-0.150	-0.089	-0.088
$Fe(s,p,d)$	-0.245	-0.117	-0.102	-0.041
$Fe(d)$	-0.023	-0.019	$+0.001$	-0.010
$Fe(2p)$	-0.002	-0.020	-0.001	-0.005
$Fe(3p)$	-0.013	$+0.150$	$+0.021$	$+0.091$
$Fe(4p)$	-0.183	-0.260	-0.102	-0.143
$Fe(p)_{total}$	-0.198	-0.130	-0.082	-0.057
monopoles external to cluster[b]	$+0.0424$		$+0.0394$	
dipoles external to cluster[b,c]	-0.0256		-0.0387	
cluster total [d]	-0.3907		-0.1647	
total V_{zz} [e]	-0.3739 a.u. = -3.63×10^{17} V/cm^2		-0.1640 a.u. = -1.59×10^{17} V/cm^2	

[a]The electronic total equals the sum of the α or β electrons. This sum also includes overlap terms.
[b]Mulliken charges are used for the ionic charges outside the cluster.
[c]We have made use of $\gamma_\infty(Fe^{3+})=-9.1$ (Ref. 31) and $\alpha_D=0.4$ Å^3 for $ZnAl_2O_4$ and $\alpha_D=0.8$ Å^3 for $ZnFe_2O_4$.
[d]The cluster total equals the combined contributions from nuclear charges, α electrons, and β electrons.
[e]The total V_{zz} equals the combined contributions from external monopoles, external dipoles, and the cluster total.

The ratio of these two results is then 1.9 ± 0.3, which is independent of $Q(^{67}Zn)$. Using $Q(^{67}Zn)=0.15$ b and the total V_{zz} given in Table V, we predict that e^2qQ is -10.8 and -4.2 MHz for $ZnAl_2O_4$ and $ZnFe_2O_4$, respectively. These theoretical results, especially that for $ZnAl_2O_4$, are in very good agreement with the experimental nuclear quadrupole coupling constants. The ratio of the theoretical V_{zz} is $0.3062/0.1201=2.5$, in fair agreement with the ratio of experimental nuclear coupling constants of 1.9 ± 0.3.

The theoretical $e^2qQ(^{67}Zn)$, obtained using the total V_{zz} found by the Hartree-Fock cluster procedure and $Q(^{67}Zn)=0.15$ b are in very good agreement with the experimental results in regards to both magnitude and sign. This good agreement is somewhat surprising, considering that Zn^{2+} is a charged defect with respect to the pure spinel $+3$ B-site ion in $ZnAl_2O_4$ and $ZnFe_2O_4$. The agreement is better for $ZnAl_2O_4$ than for $ZnFe_2O_4$, but the difference between theory and experiment may not be too serious considering the relative smallness of the e^2qQ involved for $ZnFe_2O_4$ compared to the contributions from the external monopoles and dipoles. Also, the lattice distortion introduced by the impurity Zn^{2+} is likely to be different for the two systems. However, the relative closeness between the experimental and theoretical e^2qQ results indicates that the lattice is not too distorted by the presence of the Zn^{2+} impurity at the B site. The oxygen octahedron surrounding the Zn thus appears to be quite stiff. Polarization of the oxygen anions due to the charged defect within the $(ZnO_6)^{10-}$ cluster is included self-consistently in our Hartree-Fock cluster calculations.

Finally, the results of our unrestricted Hartree-Fock (UHF) cluster investigations for the remaining two systems, Fe^{3+} at the B sites in $ZnAl_2O_4$ and $ZnFe_2O_4$, are now presented (see Table VI). The latter system corresponds to the pure $ZnFe_2O_4$ spinel, and the former to Fe^{3+} replacing Al^{3+} as a substitutional impurity. The clusters are $(FeO_6)^{9-}$ surrounded by point charges located at lattice sites for the pure spinels, with charges scaled from the formal ionic charges by the factor 2.3/3.0 as described above.

Starting with Fe^{3+} at the Al site in $ZnAl_2O_4$, the contributions to V_{zz} from within the $(FeO_6)^{9-}$ cluster consist of $+0.2397$, -0.3424, and -0.2880 a.u. due to the nuclei, α electrons (spin-up electrons), and β electrons (spin-down electrons), respectively. It appears that the α electrons contribute approximately 0.05 a.u. more to V_{zz} than the β electrons. The sum of the nuclear and electronic contributions to V_{zz} comes out to -0.3907 a.u. To obtain the total V_{zz} at the Fe nucleus, the contributions due to the external monopoles ($+0.0424$ a.u.) and dipoles (-0.0256 a.u.) must also be added to the cluster total. The total V_{zz} at the Fe nucleus is -0.3739 a.u.

Following the same procedure as above, for $ZnFe_2O_4$, whose contributions to V_{zz} at the Fe nucleus are also listed in Table VI, we find that the cluster (nuclear plus electronic), external monopole and external dipole contributions to V_{zz} are -0.1647, $+0.0394$, and -0.0387 a.u., respectively. Therefore, the total V_{zz} at the Fe nucleus in $ZnFe_2O_4$ is -0.1640 a.u.

Direct comparison with experimental nuclear quadrupole coupling constants is difficult without a reliable value for $Q(^{57}Fe)$. However, we can confidently compare our calculated field gradients to the ratio of the two experimental quadrupole couplings, since these ratios are independent of Q. The ratio of theoretical V_{zz} for Fe in $ZnAl_2O_4$ and $ZnFe_2O_4$ of 2.3 is in excellent agreement with the experimental[8,17] ratio of 2.34 ± 0.01. One may argue that this agreement is somewhat fortuitous due to the fact that one system (Fe^{3+} in $ZnFe_2O_4$) corresponds to the pure spinel, while the other system (Fe^{3+} in $ZnAl_2O_4$) corresponds to a defect spinel. In the latter situation one may expect impurity-induced lattice relaxation to influence the experimental e^2qQ significantly. However, it is likely that the distortion associated with substituting Fe^{3+} for Al^{3+} is even less than the case for substituting Zn^{2+} for Al^{3+}, the latter situation corresponding to a charged defect. The excellent agreement between experimental and theoretical nuclear quadrupole couplings for Zn^{2+} replacing either Al^{3+} in $ZnAl_2O_4$ or Fe^{3+} in $ZnFe_2O_4$ provides indirect support that the lattice is not very much distorted by the defect from that for the pure spinels.

The experimental quadrupole couplings $e^2qQ(^{57}Fe)$ can be combined with the theoretical V_{zz} results at the ^{57}Fe nucleus to estimate a value for $Q(^{57}Fe)$. We predict from our calculations that $Q(^{57}Fe)$ is close to $+0.20$ b. Both the pure spinel (Fe^{3+} in $ZnFe_2O_4$) and the defect spinel (Fe^{3+}, replacing Al^{3+} in $ZnAl_2O_4$) lead to quadrupole moments which differ by just 0.01 b. These results are inconsistent in regards to the magnitude of $Q(^{57}Fe) \approx 0.08$ b obtained by Duff, Mishra, and Das[49] from UHF calculations on iron dihalides, but are in reasonable agreement with the larger quadrupole moments $Q \sim 0.15-0.20$ b obtained by other researchers.[46–48] Due to the very good agreement found between experimental and theoretical e^2qQ for the systems Zn^{2+} and Al^{3+} at the Al site in $ZnAl_2O_4$ and Zn^{2+} at the Fe site in $ZnFe_2O_4$, as well as the excellent agreement found between ratios of experimental e^2qQ and theoretical V_{zz} for Zn and Fe at the B sites in both spinels, one is led to the conclusion that $Q(^{57}Fe) \approx 0.20$ b. This value is close to the result $Q(^{57}Fe) = 0.16$ b from a recent study of EFG's in a number of iron compounds by a band-structure procedure.[50] We are currently involved in a reassessment of the calculated EFG's (Ref. 49) in iron dihalides trapped in rare gas solids, from which the earlier lower value of Q had been obtained.

2. Individual atomic orbital contributions to the electric-field gradient at Zn and Fe

Table V lists individual atomic-orbital contributions to V_{zz} from our cluster calculations with Zn^{2+} substituting for Al^{3+} in $ZnAl_2O_4$, and with Zn^{2+} substituting for Fe^{3+} in $ZnFe_2O_4$. Here we denote the former system as Zn^{2+}: $ZnAl_2O_4$ and the latter system as Zn^{2+}: $ZnFe_2O_4$, for convenience. Beginning with Zn^{2+}: $ZnAl_2O_4$, Mulliken population analysis yielded a zinc charge of $+1.80$ for this cluster, indicating that there is a small but significant transfer of electrons from the oxygen ligands to zinc which would have a charge of $+2$ otherwise. The effect of this transfer is shown below for the zinc p-orbital contributions to V_{zz}. The net cluster V_{zz}, due to the electrons and nuclei within the $(ZnO_6)^{10-}$ cluster, came out as -0.3104 a.u. The approximate atomic-orbital contributions obtained by the procedure described in Sec. II and for ^{27}Al in $ZnAl_2O_4$ in Sec. III A give -0.284 and -0.021 a.u. for the Zn(p) and Zn(d) electrons, respectively. The sum of these two contributions to V_{zz} amounts to -0.305 a.u., which is very close to the total cluster contribution of -0.3104 a.u. The contributions from the Zn($2p$), Zn($3p$), and Zn($4p$) atomic orbitals are -0.022, -0.002, and -0.260 a.u., respectively. The Zn($4p$) electrons dominate V_{zz} at the Zn nucleus, being about 92% of the Zn(p) contribution. The total V_{zz} at the nucleus is the sum of the total cluster and external contributions, and results from the transfer of electrons from the ligand oxygen ions to the $4p$ orbitals, which would be empty in a free Zn^{2+} ion. The contributions from the external monopoles and dipoles are opposite in sign, and nearly cancel each other. The total V_{zz} is -0.3062 a.u., which is composed of -0.3104 and $+0.0042$ from sources within and external to the $(ZnO_6)^{10-}$ cluster, respectively. The total V_{zz} originates mainly from the valence Zn($4p$) electrons, which make up $\sim 85\%$ of this total with an additional $\sim 7\%$ each from Zn($3d$,$4d$) electrons and core Zn($2d$) electrons. For Zn^{2+}: $ZnAl_2O_4$, the core Zn($3p$) electrons contribute less than 1% to the total V_{zz}.

Moving next to Zn^{2+}: $ZnFe_2O_4$, we find that the total V_{zz} at the Zn nucleus, equal to -0.1201 a.u., is composed of -0.1016 and -0.0185 a.u. from sources within and external to the $(ZnO_6)^{10-}$ cluster, respectively. The Zn Mulliken charge for this cluster came out as $+1.73$. The total V_{zz} for this system is dominated again by the valence Zn($4p$) electrons, which contribute approximately -0.140 a.u. Other significant contributions are also due to the Zn(d) and the core Zn($3p$) electrons, which contribute $+0.013$ and $+0.047$ a.u., respectively, to the total V_{zz}.

In comparing the two systems Zn^{2+}: $ZnAl_2O_4$ and Zn^{2+}: $ZnFe_2O_4$, we find that, for both systems, the valence Zn($4p$) atomic orbitals are the most important in determining the total V_{zz} at the zinc nucleus. However, in the case of $ZnAl_2O_4$ the Zn($4p$) contribution is about 0.05 a.u. less than the total cluster V_{zz}, while for $ZnFe_2O_4$ the Zn($4p$) contribution is about 0.04 a.u. greater than the cluster V_{zz}. These differences are due primarily to differences in the core Zn($2p$,$3p$) contribution to V_{zz}, which is negative for Zn^{2+}: $ZnAl_2O_4$ and positive for Zn^{2+}: $ZnFe_2O_4$. It is difficult to surmise the origin of the nature of these small but significant differences.

Finally, we discuss the results for the atomic-orbital contributions to V_{zz} of our UHF calculations on the $(FeO_6)^{9-}$ clusters for Fe^{3+} at the B sites in $ZnAl_2O_4$ and $ZnFe_2O_4$. The former case corresponds to a substitutional impurity, and the latter to the pure spinel. These results are summarized in Table VI. The charges of the central Fe atoms in these clusters came out as $+2.35$ and $+2.22$, respectively, for

$ZnAl_2O_4$ and $ZnFe_2O_4$. These charges are quite close to the value of $+2.32$ found for Al in $ZnAl_2O_4$. Since the molecular orbitals are obtained from UHF calculations, the α and β electrons are in orbitals which are allowed to have different spatial wave functions. Since the $(FeO_6)^{9-}$ cluster has a total spin of 2.5, the self-consistent α and β molecular orbitals are different in general due to exchange interaction, especially between electrons in the unpaired spin orbitals in α spin state and those in the α states of the paired orbitals. One observes several interesting trends in comparing the contributions to V_{zz} from either the α or β electrons of a given individual atomic orbital. First of all, the α and β oxygen O(s,p,d) contributions are nearly the same. This is not unexpected, since O^{2-} anions are closed-shell systems with equal numbers of α and β electrons. For the Fe atomic orbitals, significant differences can be seen between the contributions from α and β electrons to V_{zz}: These differences can be understood by noting that the free Fe^{3+} cation has five spin-up (α) electrons and zero spin-down (β) electrons in the $3d$ shell. There are no $4s$, $4p$, or $4d$ electrons in the free Fe^{3+} ion; however, in the solid charge transfer from the $2s$ and $2p$ O^{2-} atomic orbitals to the empty valence orbitals, in particular the $4s$, $4p$, and β-$3d$ orbitals of iron can occur. As can be noticed in Table VI, in both spinels the dominant contribution to V_{zz} at the Fe nucleus is due to the Fe(p), especially the Fe$(3p)$ and valence Fe$(4p)$ electrons, with Fe$(4p)$ being the dominant contribution. Again the negative sign of V_{zz} and hence e^2qQ is determined by the dominant negative contribution from the cation valence p electrons. Covalency and charge-transfer effects are most important in determining both the magnitude and sign of V_{zz} in these sytems. However, the Fe$(3p)$ orbital also contributes significantly to V_{zz}, especially the β-Fe$(3p)$ electrons.

Let us first consider Fe^{3+}: $ZnAl_2O_4$. The contributions to V_{zz} from the Fe(p) and Fe(d) atomic orbitals, -0.328 and -0.042 a.u., respectively, give a total of -0.370 a.u. from these two sources. This sum of the Fe(p) and Fe(d) sources is quite close to the total V_{zz} (cluster plus external) of -0.3739 a.u. The Fe(p) and Fe(d) electrons, respectively, contribute $\sim$88% and $\sim$11% to the total V_{zz}. The α-Fe(p) contribution is substantially greater than the total β-Fe(p) contribution, even though the dominant Fe$(4p)$ contribution is 1.4 times greater for the β electrons. The β-Fe$(3p)$ electrons make a substantial positive contribution to V_{zz} which is much greater in magnitude than that from the α-Fe$(3p)$ electrons.

Moving to Fe^{3+} in $ZnFe_2O_4$, as seen in Table VI, the relative contributions to V_{zz} are similar to the case for Fe^{3+}: $ZnAl_2O_4$. That is, the Fe(p) electrons, especially the Fe$(3p)$ and Fe$(4p)$, are most important in determining the sign and magnitude of V_{zz} at the Fe nucleus. The Fe$(4p)$ orbitals make the largest contribution and determine the negative sign for V_{zz}. However, a fairly sizable contribution from the Fe$(3p)$ electrons of opposite sign reduces the magnitude of V_{zz}. For both Fe^{3+}: $ZnAl_2O_4$ and Fe^{3+}: $ZnFe_2O_4$, the β-Fe$(4p)$ and β-Fe$(3p)$ contributions to V_{zz} are greater in magnitude than the respective contributions from the α electrons. This is likely due to the relative difference in shielding by the Fe$(3d)$ electrons. There are a number of trends to observe for Fe^{3+} at the B site in both spinels. There is a substantial contribution to V_{zz} from the β-Fe$(3p)$ electrons which is opposite in sign from an even greater β-Fe$(4p)$ contribution. The ratio of these two contributions is similar in both spinels, namely 1.7 and 1.6 for $ZnAl_2O_4$ and $ZnFe_2O_4$, respectively. The Fe(d) contribution to V_{zz}, on the other hand, is fairly small. In the case of Fe^{3+}: $ZnAl_2O_4$ the Fe(d) orbitals contribute roughly 11% to the total V_{zz}, and there is no significant difference between the contributions from the α or β electrons, in sharp contrast to the Fe(p) atomic orbitals. For Fe^{3+}: $ZnFe_2O_4$, the Fe(d) orbitals contribute an even smaller relative proportion to the total V_{zz}. However, this should not imply that there is no charge transfer to the β-Fe$(3d)$ orbitals which are empty for the free Fe^{3+} cation. As seen in Table VII, which lists the gross atomic-orbital populations from a Mulliken population analysis, there is a charge transfer of $\sim$0.29 and $\sim$0.24 electrons to the β-Fe(d) orbitals in $ZnAl_2O_4$ and $ZnFe_2O_4$, respectively. We cannot distinguish between the numbers of electrons in Fe$(3d)$ and Fe$(4d)$ in this type of analysis, but most likely the majority of the transfer is to the Fe$(3d)$ atomic orbital. Since the Fe$(3d)$ contribution to V_{zz} is relatively small, one concludes that the charge distribution of the β-Fe$(3d)$ orbitals must be close to spherically symmetric. The origin of the substantial difference predicted between the individual contributions to V_{zz} from the β-Fe $(3p)$ and β-Fe$(4p)$ orbitals, and the difference between the Fe(p) α and β contributions is difficult to ascertain. We suspect, however, that due to the nearly empty β-Fe$(3d)$ shell compared to the full α-Fe$(3d)$ shell, the β-Fe$(3p)$ electrons are more polarizable than the α-Fe$(3p)$ electrons the latter being more tightly bound because of the attractive exchange interactions with the α-Fe$(3d)$ electrons. Therefore, the semicore β-Fe$(3p)$ electrons would be subjected to a greater Sternheimer antishieldinglike effect than the α orbitals.

TABLE VII. Mulliken gross populations for iron from the $(FeO_6)^{9-}$ cluster for iron at the B site in $ZnAl_2O_4$ and $ZnFe_2O_4$. The external charges are scaled ($\times$2.3/3.0) charges.

		number of electrons			
Spinel	Contribution	s	p	d	total
$ZnAl_2O_4$	α electrons	3.18	6.00	5.02	14.20
	β electrons	3.16	6.00	0.29	9.45
	$(\alpha+\beta)$	6.34	12.00	5.31	23.65
	$(\alpha-\beta)$	0.02	0.00	4.73	4.75
$ZnFe_2O_4$	α electrons	3.20	6.07	5.02	14.29
	β electrons	3.19	6.06	0.24	9.49
	$(\alpha+\beta)$	6.39	12.13	5.26	23.48
	$(\alpha-\beta)$	0.01	0.01	4.78	4.80

C. ^{57}Fe magnetic hyperfine fields

The magnetic hyperfine field at the ^{57}Fe nucleus, B_{hf}, arises from two contributions, the Fermi contact term B_C and the dipolar contribution B_D. The contact term due to the unpaired spin density at the iron nucleus is (in T) (Refs. 11 and 51)

TABLE VIII. Individual atomic-orbital contributions to the electron density at the Fe nucleus located at the B site in $ZnAl_2O_4$. $\rho_{tot}(0)=\rho(0)\uparrow+\rho(0)\downarrow$.

Orbitals	$\rho(0)\uparrow$	$\rho(0)\downarrow$	$\rho(0)\uparrow$-$\rho(0)\downarrow$	$\rho_{tot}(0)$
Fe($1s$)	5228.05	5228.14	−0.09	10 456.19
Fe($2s$)	508.22	511.72	−3.50	1019.94
Fe($3s$)	72.17	69.90	+2.27	142.07
Fe($4s$)	1.85	1.80	+0.05	3.65
Total	5810.29	5811.56	−1.27	11 621.85

$$B_C=52.4\rho_s(0) \tag{3}$$

where $\rho_s(0)$ is the spin density [the difference between spin-up (α) and spin-down (β) electron density] in units of a_0^{-3} at the iron nuclei. The α and β charge densities are given in Tables VIII and IX. The dipolar contribution to the hyperfine field, which is axially symmetric in the [111] direction, is given (in units of T) by

$$B_D=6.3(V_{zz\uparrow}-V_{zz\downarrow}) \tag{4}$$

where $V_{zz\uparrow}$ and $V_{zz\downarrow}$ are the α and β electronic contributions to V_{zz} in a.u. The total hyperfine field is $B_{hf}=B_C+B_D$. Our results for ^{57}Fe in $ZnAl_2O_4$ and $Zn^{57}Fe_4O_4$ are very similar, in fact to three significant figures the dominant Fermi contact contribution is identical for both systems. Also, since magnetic hyperfine experimental data are available only for the pure spinel $ZnFe_2O_4$, we have chosen to discuss just those results for simplicity. Using Eqs. (3) and (4), the results for $\rho_s(0)=\rho(0)\uparrow-\rho(0)\downarrow$ listed in Tables VIII and IX and the results for the α and β electronic contributions to V_{zz} listed in Table VI, we find that $B_C=-66.6$ T and $B_D=-0.1$ T. The contact contribution is much greater than the dipolar contribution which is typical for ferric compounds. The magnetic hyperfine field B_{hf} from the Hartree-Fock cluster calculations is therefore −66.7 T. A substantial correction is expected from relativistic and correlation effects to the contact contribution. We obtain estimates for these corrections from atomic many-body calculations.

A nonrelativistic many-body calculation[52] on the Fe^{3+} ion has shown that correlation reduces the magnitude of the contact contribution by 8% including consistency effects. While there are no relativistic many-body calculations on iron available, such calculations have been performed for the manganese atom.[53] First-principles many-body calculations on the manganese atom have shown that the nonrelativistic contact contribution is reduced in magnitude by 17% due to relativistic effects. Thus we correct our Hartree-Fock cluster calculations for B_{hf} in $ZnFe_2O_4$ to include relativistic and many-body effects by reducing the Hartree-Fock cluster result by 25%. This procedure gives a magnetic hyperfine field of −50.0 T at the iron nucleus in $ZnFe_2O_4$. This estimate is in very good agreement with the experimental measurement[54] of −51.5 T, extrapolated to 0 K. We emphasize, however, that this good agreement may be fortuitous due to the relatively large corrections from many-body and relativistic effects to $\rho_s(0)$ which have been taken from atomic calculations.

TABLE IX. Individual atomic-orbital contributions to the electron density at the Fe nucleus located at the B site in $ZnFe_2O_4$. $\rho_{tot}(0)=\rho(0)\uparrow+\rho(0)\downarrow$.

Orbitals	$\rho(0)\uparrow$	$\rho(0)\downarrow$	$\rho(0)\uparrow$-$\rho(0)\downarrow$	$\rho_{tot}(0)$
Fe($1s$)	5228.06	5228.15	−0.09	10 456.21
Fe($2s$)	508.24	511.75	−3.51	1019.99
Fe($3s$)	72.31	70.05	+2.26	142.36
Fe($4s$)	1.54	1.47	+0.07	3.01
Total	5810.15	5811.42	−1.27	11 621.57

TABLE X. Individual atomic-orbital contributions to the electron density at the nucleus for the Fe^{3+} free ion in atomic units (a_0^{-3}). $\rho(0)\uparrow$:$\rho(0)$ of α electrons. $\rho(0)\downarrow$:$\rho(0)$ of β electrons.

Orbitals	$\rho(0)\uparrow$	$\rho(0)\downarrow$	$\rho(0)\uparrow$-$\rho(0)\downarrow$	$\rho_{tot}(0)$[a]
Fe($1s$)	5228.11	5228.20	−0.09	10 456.31
Fe($2s$)	508.22	511.86	−3.64	1020.08
Fe($3s$)	72.63	70.34	+2.29	142.97
Total	5808.96	5810.40	−1.44	11 619.36

[a] $\rho_{tot}(0)=\rho(0)\uparrow+\rho(0)\downarrow$.

It is useful to make a comparison between the $\rho_s(0)$ for the $(FeO_6)^{9-}$ cluster representative of $ZnFe_2O_4$ and the free Fe^{3+} ion. The difference between the cluster calculation and the free-ion results can be considered as a contribution to the hyperfine field from the solid-state environment. Table X gives $\rho_s(0)$ for the $Fe^{3+}(^6S)$ ion from atomic Hartree-Fock calculations employing the same basis set as used in the cluster calculations. These results yield −75.5 T for the free-ion hyperfine field. Comparing this with $B_{hf}=-66.7$ T from the Hartree-Fock cluster calculations gives +8.8 T for the contribution to B_{hf} from the solid-state environment. Reducing this result by 25% to correct approximately for relativistic and many-body effects gives an estimate of +6.6 T for the corrected contribution to B_{hf} due to solid state effects.

The local magnetic moment has also been measured[55] by neutron-scattering experiments to be $4.2\mu_B$ for iron in $ZnFe_2O_4$, reduced from the free Fe^{3+}-ion value of $\sim 5.9\mu_B$, the reduction being ascribed to covalency effects. The Mulliken population analysis for the cluster molecular orbitals can be used to obtain a semiquantitative estimate of the difference between spin-up and spin-down electron populations within the iron atom. These results, given in Table VII, are labeled ($\alpha-\beta$) for the difference in spin-up and spin-down populations. For $ZnFe_2O_4$, we obtain $4.80\mu_B$ for the local magnetic moment, with the reduction due mainly to an increase in the minority-spin Fe($3d$) population from zero electrons for the Fe^{3+} ion to 0.24 electrons. The reduction of $\sim 1\mu_B$ while likely due to covalency effects, significantly underestimates the experimental delocalization reduction of $\sim 1.7\mu_B$.

D. Total electron density at the iron nucleus: ^{57}Fe isomer shifts

In Mössbauer spectroscopy, the isomer shift S between two different compounds is related to the charge density difference at the nucleus between the same two compounds by

TABLE XI. Theoretical $\rho(0)$, S, and S_{SOD}, as well as experimental S_C for ^{67}Zn in $Zn[Al_2O_4]$ and $Zn[Fe_2O_4]$.

Spinel	Zn site	Cluster [a]	d_{nn} (Å)[b]	Total[c] $\rho(0)$ (a_0^{-3})	Theoretical[d] S (μm/s)	Experimental[e] S_C (μm/s)	Calculated[f] S_{SOD} (μm/s)
$ZnAl_2O_4$	*A*	$(ZnO_4)^{6-}$	1.9442[g]	17 992.33	-16 ± 6	-13.0	$+3\pm6$
	B	$(ZnO_6)^{10-}$	1.9160	17 992.45	-12 ± 6	-26.5	-14 ± 6
$ZnFe_2O_4$	*A*	$(ZnO_4)^{6-}$	1.9708	17 991.96	-31 ± 6	-6.0	$+24\pm6$
	B	$(ZnO_6)^{10-}$	2.0378	17 992.02	-28 ± 6	-18.5	$+9\pm6$

[a]Scaled ($\times 2.3/3.0$) charges are used for the external point charges.
[b]Nearest-neighbor Zn-O distance.
[c]$\pm 0.10a_0^{-3}$ uncertainty.
[d]Calculated relative to ZnO (wurtzite); $\rho(0)_{ZnO}=17\,992.76\pm0.10a_0^{-3}$. S (μm/s)$=\alpha_{HF}\,\Delta\rho(0)$; $\alpha_{HF}=+(38.2\pm3.8)a_0^3$ μm/s; Ref. 20.
[e]References 18 and 19; relative to the ^{67}ZnO (wurtzite) source.
[f]Relative to ZnO (wurtzite); $S_{SOD}=S_C$(experimental)$-S$(theoretical).
[g]A slightly different u-parameter (0.3889) value was used ($u=0.3887$ would give $d_{nn}=1.9414$ Å, a decrease of 0.14%).

$$S=\alpha_{HF}[\rho_1(0)-\rho_2(0)], \tag{5}$$

where α_{HF} is known as the isomer shift calibration constant. If S is in mm/s, $\rho(0)$ in a_0^{-3}, then α_{HF} is in units of (mm/s)a_0^3. For ^{57}Fe, and $\rho(0)$ obtained from nonrelativistic calculations, a current estimate[30,56,57] of α_{HF} is -0.27 (mm/s)a_0^3. If $\rho_1(0)$ is the charge density at the iron nucleus for Fe^{3+}: $ZnAl_2O_4$, and $\rho_2(0)$ refers to $ZnFe_2O_4$, then from Tables VIII and IX we find that $\rho_1(0)-\rho_2(0)=0.28a_0^{-3}$. From Eq. (5) we predict that the isomer shift between these systems is about -0.08 mm/s. The higher charge density at the Fe nucleus for $ZnAl_2O_4$ as compared to $ZnFe_2O_4$ is due to the shorter Fe-O bond length in the former. Our results predict a greater covalency for Fe^{3+}: $ZnAl_2O_4$ than for $ZnFe_2O_4$. Using the experimental isomer shifts[17,8] for $ZnAl_2O_4$ and $ZnFe_2O_4$ with respect to iron metal of $+0.32$ and $+0.35$ mm/s, respectively, the experimental isomer shift between the two spinels is -0.03 mm/s. The correct sign and approximate magnitude (small) is predicted by our theoretical results for the charge densities. Based on typical uncertainties[20] in calculated $\Delta\rho(0)$ of about $\pm0.1a_0^{-3}$ for Hartree-Fock calculations with Gaussian basis sets, these results are reasonable.

Perhaps a better comparison can be made with systems which have much larger isomer shifts between them, and for which theoretical $\rho(0)$ calculations are available. Nieuwport, Post, and van Duijnen[57] have calculated $\Delta\rho(0)$ at the iron nucleus for a relatively large number of ferrous and ferric compounds as well as the free ions $Fe^{2+}(^5D)$ and $Fe^{3+}(^6S)$ with the same basis sets. Using their result for the ferrous system $K_3Fe(CN)_6$ gives

$$\rho[Fe^{3+}]-\rho[K_3Fe(CN)_6]=-4.26a_0^{-3}.$$

For our calculations from Tables IX and X, we obtain

$$\rho[Fe^{3+}]-\rho[ZnFe_2O_4]=-2.21a_0^{-3}.$$

Therefore, the density difference between the two compounds is

$$\Delta\rho(0)=\rho[ZnFe_2O_4]-\rho[K_3Fe(CN)_6]=-2.05a_0^{-3},$$

from which the isomer shift between them is predicted to be $+0.55$ mm/s. The experimental isomer shifts, with respect to iron metal, for (Ref. 8) $ZnFe_2O_4$ and (Ref. 58) $K_3Fe(CN)_6$, are 0.35 and -0.13 mm/s, respectively. Therefore, the experimental isomer shift between the two compounds is then $+0.48$ mm/s, which is in satisfactory agreement with our theoretical result of $+0.55$ mm/s. The difference between these two results of 0.07 mm/s is about 15% of the experimental isomer shift between these two compounds.

E. Total electron density at the zinc nucleus located at *A* and *B* sites in $ZnAl_2O_4$ and $ZnFe_2O_4$

In addition to the situation when zinc is a substitutional impurity at the *B* site, we have calculated the total electron density $\rho(0)$ for zinc at the *A* sites as well. This latter case corresponds to the pure spinel. The basis sets are the same as used earlier for electric-field gradients at the zinc nucleus. The external charges are all scaled ($\times 2.3/3.0$) from the formal charges as before. The chosen cluster for the tetrahedrally coordinated *A* site is $(ZnO_4)^{6-}$. The $(ZnO_6)^{10-}$ cluster for the *B* site is the same as described earlier. In fact, the results for $\rho(0)$ at the zinc nucleus are calculated from the molecular orbitals from the earlier study. The results for the total charge density at the zinc nucleus for the pure *A* site and substitutional *B* site (without lattice relaxation) for both spinels are given in Table XI. Also, presented are recently[18,19] available ^{67}Zn Mössbauer center shifts, S_C, with respect to a ^{67}ZnO source. One should recall that, for ^{67}Zn Mössbauer effect, unlike ^{57}Fe, the second-order Doppler effect (SOD) cannot be ignored. It is possible that most of S_C, which is the sum of the isomer shift S and the shift S_{SOD}, is due to the second-order Doppler effect. Unlike ZnF_2 and the zinc chalcogenides[20] ZnO, ZnS, ZnSe, and ZnTe, there currently is no reliable calculation for S_{SOD} in spinels. We therefore cannot make a direct comparison between our calculated $\rho(0)$ and S_C.[20] We can only make predictions for S_{SOD} from our theoretical results combined with the experimental S_C. Finally, Table XII gives results for individual contributions to $\rho(0)$.

TABLE XII. Individual contributions to $\rho(0)$ at the ^{67}Zn nucleus.

	$\rho(0)(a_0^{-3})$[a]			
Orbitals	$ZnAl_2O_4$ *A* site[b]	$ZnAl_2O_4$ *B* site[c]	$ZnFe_2O_4$ *A* site[b]	$ZnFe_2O_4$ *B* site[c]
Zn(1*s*)	16 116.19	16 116.18	16 116.21	16 116.21
Zn(2*s*)	1639.12	1639.07	1639.13	1639.11
Zn(3*s*)	234.37	234.11	234.36	234.26
Zn(4*s*)	2.65	3.09	2.26	2.44
Total	17 992.33	17 992.45	17 991.96	17 992.02

[a]Scaled ($\times 2.3/3.0$) charges are used for the external charges.
[b]$(ZnO_4)^{6-}$ cluster.
[c]$(ZnO_6)^{10-}$ cluster.

From our previous study of the pressure dependence of the isomer shift for the cubic zinc chalcogenides,[19] our results predicted that $\rho(0)$ at the zinc nucleus increased with decreasing zinc-ligand nearest-neighbor distance. As seen in Table XI, the same trend is seen for $\rho(0)$ when looking at either the *A* or *B* site. First, let us compare the *A* sites. In going from $ZnAl_2O_4$ to $ZnFe_2O_4$, d_{nn} increases by about 1.4%, while $\rho(0)$ decreases by $0.37a_0^{-3}$. We estimate, based on our previous work[20] on ^{67}Zn isomer shifts in binary zinc compounds, that the error in calculated $\Delta\rho(0)$ is approximately $\pm 0.10a_0^{-3}$. The same general trend is predicted for the *B* sites. In going from $ZnAl_2O_4$ to $ZnFe_2O_4$, d_{nn} increases by about 6.4%, while $\rho(0)$ decreases by $0.43a_0^{-3}$. Decreasing Zn-O bond lengths increases the covalency of the Zn-O bond by increasing overlap of their orbitals. The Zn(4*s*) contribution is expected to increase, and it does, as can be seen from Table XII. The Zn(3*s*) contribution partially compensates for the increase of the Zn(4*s*) density because of the Pauli exclusion principle.[20]

These predicted trends are in disagreement with measured center shifts, assuming S_C is due primarily to the isomer shift. S_C actually increases with increasing Zn-O nearest-neighbor distance when comparing either *A* or *B* sites.[19]

The isomer shift calibration constant α_{HF} for ^{67}Zn is known from our earlier work[20] as 38.2 ± 3.8 (μm/s)(a_0^3) for nonrelativistic $\Delta\rho(0)$. In Table XI we have listed theoretical *S*, relative to ZnO (wurtzite), using a result for the charge density at the zinc nucleus in ZnO from an earlier calculation[20] which employed the same methods and basis sets as here for the spinels. In all cases the spinels are predicted to have negative *S* with respect to ZnO (wurtzite). This is in agreement with the trends for experimental S_C, though the magnitudes vary quite a bit.

From Table XI, we predict that between the *A* sites $S(A$ sites) is $+(15\pm 8)$ μm/s and that between the *B* sites $S(B$ sites) is $+(16\pm 8)$ μm/s, where $ZnAl_2O_4$ has the greater charge density at the zinc nucleus in both cases. The relative isomer shifts between $ZnAl_2O_4$ and $ZnFe_2O_4$ are thus predicted to be similar for both *A* and *B* sites.

Now, let us compare the *A* and *B* site $\rho(0)$ results for the same spinel. The *A* site is predicted by our cluster calculations to have very similar charge densities at the zinc nucleus relative to the *B* site within the same spinel. For $ZnAl_2O_4$, $\rho(A$ site$)-\rho(B$ site$)=-(0.12\pm 0.15)a_0^{-3}$, while for $ZnFe_2O_4$, $\rho(A$ site$)-\rho(B$ site$)=-(0.06\pm 0.15)a_0^{-3}$. The general trend in the experimental S_C is that, for both spinels, the center shift of the *A* site is greater than that of the *B* site by about 13 μm/s. If the center shift is due entirely to the isomer shift with $S_{SOD}=0$, then $\rho(0)$ is predicted to be $(0.34\pm 0.04)a_0^{3-}$ greater at the *A* site than the *B* site. Our theoretical results are considerably lower than this, being about zero. There are several possible reasons for these discrepancies between our calculated $\Delta\rho(0)$ and the experimental S_C. We have already mentioned the possible role of S_{SOD}. Assuming that the theoretical $\Delta\rho(0)$ are accurate then we predict (see Table XI) that the S_{SOD} are quite significant in spinels being in some cases even greater in magnitude and opposite in sign than the isomer shift contribution to S_C. Another possibility, which will be clearer when independent S_{SOD} results become available, is that the use of small (nearest neighbors only) clusters surrounded by point charges may be inadequate for accurate $\Delta\rho(0)$ calculations in spinels. This may be true for both the *A* and *B* sites in regards to charge densities at the zinc nucleus. At the *B* site, we have substituted a $+3$ *B*-site ion with the Zn^{2+} ion. The zinc defect is therefore a charged defect unlike the case where Fe^{3+} substituted for Al^{3+} in $ZnAl_2O_4$. In regards to the *A* site, corresponding to the pure spinel, the *A* site is surrounded by 12 second-nearest-neighbor $+3$ ions (actually $+2.3$ since scaled charges are used). Therefore, the nearest-neighbor oxygens to the *A* site may be subjected to a potential which is quite sensitive to the surrounding point charges. However, our results on the nuclear quadrupole interactions (see Sec. III B) showed that the lattice is not very much distorted by the presence of the Zn^{2+} impurity at the *B* site. For this reason we expect the influence of the charged zinc defect on $\Delta\rho(0)$ to be quite small.

A final consideration is that significant covalent mixing can be expected between the *A* and *B* site cations, at least in $ZnFe_2O_4$. It is known that $ZnFe_2O_4$ orders antiferromagnetically at 10 K. Below 10 K a transferred (via oxygen ligands) hyperfine field $B_{thf}\approx 1$ T is observed at the Zn nucleus.[18,19,59] The possibility of *A*-*B* interactions involving covalency through the oxygens is obviously not included in nearest-neighbor clusters. Much larger clusters would be needed to study the influence of such effects on $\rho(0)$.

At present it is not possible to exclude any of the possibilities mentioned. In ^{67}Zn-Mössbauer spectroscopy S_{SOD} often is a significant contribution to the observed center shift S_C (Ref. 60), and might well be responsible for the discrepancies described above.

IV. CONCLUSIONS

The first-principles all-electron Hartree-Fock cluster procedure is applied to the compounds $ZnAl_2O_4$ and $ZnFe_2O_4$, for the pure spinels Zn^{2+} and Fe^{3+} substituted for Al^{3+} in $ZnAl_2O_4$ and Zn^{2+} substituted for Fe^{3+} in $ZnFe_2O_4$. Electric-field gradients are calculated at the *B*-site nuclei using clusters which involve the *B*-site cation and its six nearest-neighbor oxygens. The rest of the solid is included by considering all sites outside the cluster as point ions. The calculated electric-field gradients agreed well with the available NQI data. For the impurity system, the possibility of impurity-induced lattice relaxation is not included.

However, the concordance found between theoretical and experimental ^{67}Zn nuclear quadrupole coupling constants (e^2qQ) indirectly suggests that the relaxation due to the presence of the defect is relatively small. For ^{57}Fe or ^{67}Zn at the *B* site, the ratios $V_{zz}[ZnAl_2O_4]/V_{zz}[ZnFe_2O_4]$ agree very well with the corresponding ratios of experimental e^2qQ. This is significant because these ratios are independent of the nuclear quadrupole moment Q. Combined with the good agreement found between theoretical and experimental results for e^2qQ of ^{27}Al and ^{67}Zn, the present calculations suggest that $Q(^{57}\text{Fe})\approx 0.2$ b. In regards to individual contributions to V_{zz}, the *B*-site cation valence *p* orbitals are dominant. The contribution to V_{zz} from the oxygen dipole moments external to the cluster has been estimated by use of the point-dipole model. We show here that this contribution is important: it can be as large as 48% of the total V_{zz} at the *B* site.

The ^{57}Fe magnetic hyperfine field is calculated, and very good agreement is obtained with the experimental result for $ZnFe_2O_4$, after correcting the Hartree-Fock results for many-body and relativistic effects, which are found to be important. The magnetic moment of Fe in $ZnFe_2O_4$ is estimated from the Mulliken population analysis, and is found to be somewhat larger than the experimental moment. This result suggests that larger clusters are needed involving both *A* and *B* site cations to include *A*-O-*B* interactions which may reduce the Fe magnetic moment. Finally, the ^{57}Fe isomer shift between the two systems Fe^{3+}: $ZnAl_2O_4$ and $ZnFe_2O_4$ is very small, in agreement with experimental data. The calculated isomer shift between $ZnFe_2O_4$ and the ferrous compound $K_3Fe(CN)_6$ is concordant with experiment.

Theoretical charge densities at the zinc nucleus are calculated at the *A* sites for the pure spinels, and for the *B* sites when zinc is a substitutional defect. These results are difficult to directly compare with experimental ^{67}Zn Mössbauer data due to the non-negligible contribution to the center shift from the second-order Doppler (S_{SOD}) effect. Independent S_{SOD} results from lattice-dynamical calculations are not yet available for these compounds. The theoretical ^{67}Zn isomer shifts are combined with experimental ^{67}Zn center shifts to derive estimates for S_{SOD}. Hopefully, S_{SOD} will become available for spinels in the future. Our calculations suggest that contributions to the center shift from the second-order Doppler effect are significant in oxide spinels.

ACKNOWLEDGMENTS

We gratefully acknowledge the continuous support of the cyclotron group at the Forschungszentrum Karlsruhe, and would especially like to thank Dr. H. Schweickert, K. Assmus, and W. Maier. This work has been funded by the German Federal Minister for Research and Technology [Bundesminister für Forschung und Technologie (BMFT)] under Contract No. KA3TUM and the Forschungszentrum Karlsruhe.

*Present address: Pacific Northwest Laboratory, Dept. of Chemical Sciences, Richland, WA 99352.

[1] E. J. W. Verwey and E. L. Heilmann, J. Chem. Phys. **15**, 174 (1947); E. J. Verwey, P. W. Haayman, and F. C. Romeijn, *ibid.* **15**, 181 (1947).

[2] E. W. Gorter, Philips Res. Rep. **9**, 295 (1954).

[3] R. J. Hill, J. R. Craig, and G. V. Gibbs, Phys. Chem. Minerals **4**, 317 (1979).

[4] R. E. Vandenberghe and E. deGrave, in *Mössbauer Spectroscopy Applied to Inorganic Chemistry*, edited by G. J. Long and F. Grandjean (Plenum, New York, 1989), Vol. 3, p. 59.

[5] D. L. Anderson, Science **223**, 347 (1984).

[6] D. C. Johnston, H. Prakash, W. H. Zachariasen, and R. Viswanathan, Mater. Res. Bull. **8**, 777 (1973).

[7] A. Hudson and H. J. Whitfield, Mol. Phys. **12**, 165 (1967).

[8] B. J. Evans, S. S. Hafner, and H. P. Weber, J. Chem. Phys. **55**, 5282 (1971).

[9] R. Kirsch, A. Gerard, and M. Wautelet, J. Phys. C **7**, 3633 (1974).

[10] J. Sauer, Chem. Rev. **89**, 199 (1989).

[11] P. C. Kelires and T. P. Das, Hyperfine Interact. **34**, 285 (1987).

[12] H. H. Klaus, N. Sahoo, P. C. Kelires, T. P. Das, W. Potzel, G. M. Kalvius, M. Frank, and W. Kreische, Hyperfine Interact. **60**, 853 (1990).

[13] D. W. Mitchell, S. B. Sulaiman, N. Sahoo, T. P. Das, W. Potzel, and G. M. Kalvius, Phys. Rev. B **44**, 6728 (1991).

[14] S. B. Sulaiman, N. Sahoo, T. P. Das, O. Donzelli, E. Torikai, and K. Nagamine, Phys. Rev. B **44**, 7028 (1991).

[15] N. Sahoo, S. Markert, K. Nagamine, and T. P. Das, Phys. Rev. B **41**, 220 (1990).

[16] D. W. Mitchell, S. B. Sulaiman, N. Sahoo, T. P. Das, W. Potzel, G. M. Kalvius, W. Schiessl, H. Karzel, and M. Steiner, Hyperfine Interact. **78**, 403 (1993).

[17] P. Rüeggsegger, F. Waldner, and E. Brun, Helv. Phys. Acta **43**, 799 (1970).

[18] W. Schiessl, W. Potzel, H. Karzel, C. Schäfer, M. Steiner, M. Peter, G. M. Kalvius, I. Halvey, J. Gal, W. Schäfer, and G. Will, Hyperfine Interact. **68**, 161 (1991).

[19] W. Schiessl, W. Potzel, H. Karzel, M. Steiner, M. Köfferlein, G. M. Kalvius, K. Melzer, G. Dietzmann, A. Martin, I. Halevy, J. Gal, W. Schäfer, G. Will, D. W. Mitchell, and T. P. Das, Hyperfine Interact. **90**, 359 (1994).

[20] D. W. Mitchell, T. P. Das, W. Potzel, M. Köfferlein, H. Karzel, W. Schiessl, M. Steiner, and G. M. Kalvius, Phys. Rev. B **48**, 16 449 (1993).

[21] C. C. J. Roothaan, Rev. Mod. Phys. **23**, 69 (1951).

[22] K. A. Colbourn and J. Hendrick, in *Computer Simulation of Solids*, edited by C. R. A. Catlow and W. C. Mackrodt (Springer-Verlag, New York, 1982), p. 67.

[23] B. R. A. Nijboer and F. W. DeWette, Physica **23**, 309 (1957); S. Hafner and M. Raymond, J. Chem. Phys. **49**, 3570 (1968).

[24] A. Hinchliffe, *Ab Initio Determination of Molecular Properties* (Hilger, Bristol, 1987).

[25] *Gaussian Basis Sets for Molecular Calculations*, edited by S. Huzinaga, J. Andzelm, M. Klobukowski, E. Radzio-Andzelm, Y. Sakai, and H. Tatewaki (Elsevier, Amsterdam, 1984).

[26] T. H. Dunning and P. J. Hay, in *Modern Theoretical Chemistry*, edited by H. F. Schaefer (Plenum, New York, 1977), Vol. 3, Chap. 1.

[27] A. J. H. Wachters, J. Chem. Phys. **52**, 1033 (1970).

[28] D. R. Yarkony and H. F. Schaefer, Chem. Phys. Lett. **15**, 514 (1972).

[29] R. S. Mulliken, J. Chem. Phys. **23**, 1833 (1955); **23**, 1841 (1955).
[30] K. J. Duff, Phys. Rev. B **9**, 66 (1974).
[31] R. M. Sternheimer, Phys. Rev. **130**, 1423 (1963); R. M. Sternheimer, Phys. Rev. **146**, 140 (1966).
[32] R. M. Sternheimer, Z. Naturforsch. Teil A **41**, 24 (1986).
[33] T. P. Das and B. G. Dick, Phys. Rev. **127**, 1063 (1962).
[34] T. T. Taylor and T. P. Das, Phys. Rev. **133**, A1327 (1964).
[35] D. W. Mitchell, Ph.D. thesis, State University of New York at Albany, 1993.
[36] Z. M. Stadnik and W. Zarek, Phys. Rev. B **34**, 1820 (1986).
[37] P. C. Schmidt, K. D. Sen, T. P. Das, and A. Weiss, Phys. Rev. B **22**, 4167 (1980).
[38] J. E. Rodgers, R. Roy, and T. P. Das, Phys. Rev. A **14**, 543 (1976).
[39] D. Sundholm and J. Olsen, Phys. Rev. Lett. **68**, 927 (1992).
[40] S. N. Ray, Taesul Lee, and T. P. Das, Phys. Rev. A **9**, 93 (1974).
[41] S. N. Ray, Taesul Lee, and T. P. Das, Phys. Rev. B **12**, 58 (1975).
[42] E. Bominaar, J. Guillin, V. R. Marathe, A. Sawaryn, and A. X. Trautwein, Hyperfine Interact. **40**, 111 (1988).
[43] W. R. Wadt and P. J. Hay, J. Chem. Phys. **82**, 284 (1985).
[44] A. Lurio, Phys. Rev. **126**, 1768 (1962).
[45] N. S. Laulainen and M. N. McDermott, Phys. Rev. **177**, 1606 (1969).
[46] R. Ingalls, Phys. Rev. **188**, 1045 (1969).
[47] S. Lauer, V. R. Marathe, and A. Trautwein, Phys. Rev. A **19**, 1852 (1979).
[48] S. N. Ray and T. P. Das, Phys. Rev. B **16**, 4794 (1977).
[49] K. J. Duff, K. C. Mishra, and T. P. Das, Phys. Rev. Lett. **46**, 1611 (1981).
[50] P. Dufek, P. Blaha, and K. Schwarz, Phys. Rev. Lett. **75**, 3545 (1995).
[51] N. Sahoo, K. Ramani Lata, and T. P. Das, Theor. Chim. Acta **82**, 285 (1992).
[52] S. N. Ray, T. Lee, and T. P. Das, Phys. Rev. B **8**, 5291 (1973).
[53] J. Andriessen, S. N. Ray, T. Lee, D. Ikenberry, and T. P. Das, Phys. Rev. A **13**, 1669 (1976).
[54] U. König, E. F. Bertraut, and G. Chol, Solid State Commun. **8**, 759 (1970).
[55] U. König, Tech. Mitt. Krupp Forschungber. **30**, 1 (1972).
[56] D. Guenzburger, D. M. S. Esquivel, and J. Danon, Phys. Rev. B **18**, 4561 (1978).
[57] W. C. Nieuwpoort, D. Post, and P. Th. van Duijnen, Phys. Rev. B **17**, 91 (1978).
[58] L. Y. Johansson, R. Larsson, J. Blomquist, C. Cederström, S. Grapengiesser, U. Helgeson, L. C. Moberg, and M. Sundbom, Chem. Phys. Lett. **24**, 508 (1974).
[59] W. Schiessl, Ph.D. thesis, Technische Universität München, 1994.
[60] W. Potzel, in *Mössbauer Spectroscopy Applied to Magnetism and Materials Science*, edited by G. J. Long and F. Grandjean (Plenum, New York, 1993), Vol. 1, p. 305.